BBA - Biomembranes 1862 (2020) 183215

Contents lists available at ScienceDirect

BBA - Biomembranes

journal homepage: www.elsevier.com/locate/bbamem

Microfluidic diffusional sizing probes lipid nanodiscs formation

Mehdi Azouz[a], Mathilde Gonin[a], Sebastian Fiedler[b], Jonathan Faherty[b], Marion Decossas[a], Christophe Cullin[a], Sandrine Villette[a], Michel Lafleur[c], Isabel D. Alves[a], Sophie Lecomte[a,*], Alexandre Ciaccafava[a,*]

[a] Univ Bordeaux, CNRS, CBMN UMR 5248, Bat B14 Allée Geoffroy St Hilaire, F-33600 Pessac, France
[b] Fluidic Analytics Ltd, Unit A, The Paddocks Business Centre, Cherry Hinton Rd, Cambridge CB1 8DH, United Kingdom
[c] Department of chemistry, Université de Montréal, 2900, Édouard-Montpetit blvd., Montréal, Québec, Canada

ARTICLE INFO

Keywords:
Polymer nanodiscs
SMALP
Lipids
Peptide
Microfluidic diffusional sizing

ABSTRACT

The biophysical characterisation of membrane proteins and their interactions with lipids in native membrane habitat remains a major challenge. Indeed, traditional solubilisation procedures with detergents often causes the loss of native lipids surrounding membrane proteins, which ultimately impacts structural and functional properties. Recently, copolymer-based nanodiscs have emerged as a highly promising tool, thanks to their unique ability of solubilising membrane proteins directly from native membranes, in the shape of discoidal patches of lipid bilayers. While this methodology finally set us free from the use of detergents, some limitations are however associated with the use of such copolymers. Among them, one can cite the tedious control of the nanodiscs size, their instability in basic pH and in the presence of divalent cations. In this respect, many variants of the widely used Styrene Maleic Acid (SMA) copolymer have been developed to specifically address those limitations. With the multiplication of new SMA copolymer variants and the growing interest in copolymer-based nanodiscs for the characterisation of membrane proteins, there is a need to better understand and control their formation. Among the techniques used to characterise the solubilisation of lipid bilayer by amphipathic molecules, cryo-TEM, ^{31}P NMR, DLS, ITC and fluorescence spectroscopy are the most widely used, with a consensus made in the sense that a combination of these techniques is required. In this work, we propose to evaluate the capacity of Microfluidic Diffusional Sizing (MDS) as a new method to follow copolymer nanodiscs formation. Originally designed to determine protein size through laminar flow diffusion, we present a novel application along with a protocol development to observe nanodiscs formation by MDS. We show that MDS allows to precisely measure the size of nanodiscs, and to determine the copolymer/lipid ratio at the onset of solubilisation. Finally, we use MDS to characterise peptide/nanodisc interaction. The technique shows a promising ability to highlight the pivotal role of lipids in promoting interactions through a case study with an aggregating peptide. This confirmed the relevance of using the MDS and nanodiscs as biomimetic models for such investigations.

1. Introduction

The plasma membrane is a complex supramolecular assembly composed of various lipids, sugars and membrane proteins (MPs) working together to modulate essential biological processes such as generation of electrochemical gradient, signalling pathways, ligand-receptor interactions and energy conversion processes [1]. Despite the importance of this key interface crucial for life, many aspects remain obscure and rather poorly investigated. Among them, the characterisation of MPs in natural membranes remains a major challenge. Indeed the proper functionality of a MP is intimately linked to its native environment: the lipid membrane [2]. One of the main bottlenecks lies in the ability to extract MPs from their native environment while preserving their biological properties. A paradox that has considerably held back researches, as reflected by the small amount of structural data available for MPs (<1% in the Protein Data Bank (PDB)) [3]. Traditionally detergents are used to solubilise biological membranes and ultimately extract MPs prior to biophysical characterisation [4,5]. However in many cases, solubilisation with detergents leads to inactivation of the MPs. Among the reasons invocated for such a loss, the dissociation character of detergent leading to delipidation of the MPs is often pointed out.

* Corresponding authors.
E-mail addresses: s.lecomte@cbmn.u-bordeaux.fr (S. Lecomte), a.ciaccafava@cbmn.u-bordeaux.fr (A. Ciaccafava).

https://doi.org/10.1016/j.bbamem.2020.183215
Received 15 November 2019; Received in revised form 4 February 2020; Accepted 5 February 2020
Available online 12 February 2020
0005-2736/

As valuable alternative to detergent solubilisation, tailored amphipathic polymer (amphipols) have succeeded in solubilising membranes while maintaining the functionality of a wide range of MPs [6]. However, those methods fail to keep native lipids around the MP. In order to provide closer physiological conditions, reconstitution methods of MPs into biomimetic lipid bilayers of controlled compositions have been developed. Detergent solubilised MPs can be reconstituted into spherical lipid bilayer system (liposomes) or planar ring shaped lipid bilayer surrounded by a rim of short detergent molecules (bicelles) [7]. Bicelles are particularly suited for NMR studies due to their ability to align in magnetic field [8]. Closely related to bicelles, membrane scaffold protein (MSP) lipid nanodiscs are constituted of a disc-shaped lipid bilayer sizing around 10 nm diameter surrounded by a belt of MSP [9]. Unfortunately, the MSP allowing the formation of nanodiscs often interferes with spectroscopic investigations due to spectral overlap with the targeted MP.

While the aforementioned methods represent a considerable improvement, they however require the MP to be first solubilised with detergent before reconstitution into those mimicking systems. This transient state might induce irreversible structural changes and loss of essential lipids, which could act as cofactors [10]. Recently a new class of nanodiscs has emerged, characterised by the substitution of MSP by amphiphilic copolymers forming a belt around lipid bilayers [11]. Styrene Maleic – Acid (SMA) was the first copolymer to be used, with styrene as a hydrophobic moiety and maleic acid as the hydrophilic part [12]. This novel class of nanodiscs referred as SMALPs (SMA lipid particles) offers the unique feature of extracting MPs directly from the native membrane with their intimate surrounding lipids. Typically, 100–200 lipids are co-extracted [13,14]. With such approaches, MPs are solubilised in a single step without any detergent. Moreover, thanks to their unique ability, the use of SMALPs for MPs extraction and their analysis by lipidomics have revealed very distinct environments around different MPs [15,16]. SMA copolymers have been shown to efficiently solubilise membranes with various lipid compositions including prokaryotic and eukaryotic membranes [17–19]. While SMALPs open the road to a wide range of biophysical characterisation techniques, they also suffer from inherent limitations. The first one is the size of the MP that can be extracted, which is directly linked to the maximal size of the nanodisc. Typically, SMALPs have a 10 nm diameter but reported values range from 5 to 30 nm depending on the preparation and the MP extracted [20]. So far, the largest MP trapped inside a SMALP is the alternative complex III associated with a cytochrome *c* oxidase constituting a supercomplex of 464 kDa and 48 transmembrane helix [21]. In this supramolecular assembly, only 11 lipid molecules were observed, reflecting somehow a very tight packing. The second limitation is the pH range of use since SMA tends to aggregate at pH below 6.5 [22]. SMA copolymer also chelates divalent cations impeding its use under these conditions. Finally, the styrene group of SMA absorbs light at 260 nm, an absorption that can be advantageously used to quantify its concentration, but unfortunately that also overlaps with protein absorption signals.

In this respect, several variants of SMA have been designed to overcome those limitations but also to broaden their potential applications [22]. Among them, tolerance to divalent cations has been largely improved (up to 20 mM) thanks to the substitution of the styrene ring by a diisobutylene moiety (DIBMA) [23]. Thanks to the absence of the styrene ring, DIBMA copolymer and a methacrylate copolymer were shown to be compatible with UV–vis spectroscopy for protein characterisation [24]. The pH range of use has been extended down to 2.5 and up to 10 thanks to the addition of an ammonium derivative on the maleic acid part. Moreover, this modification allowed a size tunability of the nanodisc diameter from 10 to 30 nm depending on the copolymer/lipid ratio [25]. Furthermore, SMA copolymers were modified to incorporate a thiol function for click chemistry, paving the way for many applications including surface immobilisation and labelling [26].

Another bottleneck that needs further investigation regards the SMALP formation process. Indeed, only a handful of studies have addressed the problematic of SMALP formation. Among them, a systematic biophysical study has investigated SMA copolymer solubilisation of lipid bilayers of various composition, leading to the proposal of a model for SMA-driven membrane solubilisation mode of action [19]. This experimental work was further supported by coarse-grained molecular dynamics [27,28]. Together, those data are giving a clearer picture of SMALP formation mechanism. The general mechanism of membrane solubilisation by copolymer can be compared to the one followed by detergents. Thus, the formation of nanodiscs follows the so-called three-stage model and can be depicted with the use of two dimensional composition-phase diagrams [29–31]. In the stage I, the copolymer is added stepwise to the bilayers (generally in the form of large unilamellar vesicles (LUVs)) and starts interacting with the surface mostly through hydrophobic and to a lesser extent electrostatic forces. After this initial surface binding, SMA copolymer inserts into the hydrophobic membrane core in a process modulated by the alkyl chain packing. Further polymer addition leads to a saturation limit, as the bilayer can no longer incorporate the copolymer, and nanodiscs start being expelled from the membrane. The copolymer to lipid molar ratio at which this transition occurs is generally called saturation (R_{sat}) and marks the beginning of stage II. When reported on a diagram, this precise ratio represents the phase boundary between the copolymer-containing vesicle domain and the coexistence domain where nanodiscs are in equilibrium with copolymer-containing vesicles. As more copolymer is added to the vesicles, complete solubilisation occurs at a higher ratio called solubilisation (R_{sol}) corresponding to the beginning of stage III, marking the phase boundary between the coexistence range and the domain of pure nanodiscs.

Many techniques are available to follow the copolymer-induced solubilisation of lamellar vesicles. Among them, one can cite dynamic light scattering (DLS), solid state ^{31}P NMR, fluorescence spectroscopy, Cryo transmission electron microscopy (TEM), and isothermal titration calorimetry (ITC) (see [29] for a thorough review in the context of detergent solubilisation). In this work, we propose to evaluate the potential of the Microfluidic Diffusional Sizing (MDS) technology as an alternative method to follow SMALPs formation. Originally, MDS was designed to determine the size and concentration of protein samples for quality control purposes [32]. Soon after, other applications have emerged and the method has been applied to evaluate protein/ligand and protein/lipid interactions [33–35]. We have chosen to investigate the thoroughly characterised phosphatidylcholine (PC), a major lipid component of mammalian membranes. In particular, we have focused on POPC and DMPC for straightforward comparison with literature. We present a specific protocol for MDS detection of lipid self-assemblies instead of proteins, based on the introduction of a small fraction of amino-containing lipids (POPE in POPC and DMPE in DMPC) and we discuss the information extracted by MDS on SMALP formation. Our approach is supported by DLS and transmission electron microscopy (TEM) measurements. Moreover, we have used MDS along with SMALPs as lipid model system to investigate the role of a specific lipid in promoting membrane/peptide interactions in a case study. We have used K18 peptide as an example, corresponding to the aggregative domain of Tau protein, and demonstrated that MDS can highlight the role of PIP_2 in triggering such interaction.

2. Materials and methods

2.1. Materials

1-Palmitoyl-2-oleoyl-*sn*-glycero-3-phosphocholine (POPC), 1-palmitoyl-2-oleoyl-*sn*-glycero-3-phosphoethanolamine (POPE), 1,2-dimyristoyl-*sn*-glycero-3-phosphocholine (DMPE), 1,2-dimyristoyl-*sn*-glycero-3-phosphocholine (DMPC) L-α-phosphoinositol-4,5-biphosphate (PIP_2, purified from porcine brain) were purchased from Avanti Polar Lipids (Alabaster, AL) and were received as organic solutions (chloroform and

chloroform/methanol/water for PIP_2 (20:(9,1) vol/vol)). 4-(2-Hydroxyethyl)-1-piperazineethanesulfonic acid (HEPES) and sodium chloride were obtained from Sigma (Steinhem, Germany). All the solutions were prepared with ultra-pure water (18 MΩ cm).

2.2. Preparation of SMA (3,1) stock solution

SMA (3:1) (XIRAN® SL25010 P20) was a kind gift from Polyscope. SMA (3:1) in HEPES 50 mM pH 7.0 was prepared trough dialysis as described before [36]. The final concentration was determined by UV–vis spectroscopy (Jasco V630 spectrophotometer) by measurement of the absorbance at 260 nm and using a molar extinction coefficient ε_{260} = 6989 L. $mol^{-1}.cm^{-1}$ obtained elsewhere [23].

2.3. Preparation of lipid suspensions

Lipid solutions were mixed to obtain the desired molar ratio (POPC/PIP_2, 80:20% mol), or weight ratio (POPC/POPE (9:1), DMPC/DMPE (9:1)). Organic solvents were then evaporated under a gentle stream of nitrogen to form lipid films. In case of mixtures, evaporation was carried out at 50 °C to ensure lipids miscibility. To remove residual solvent traces, the lipid films were further dried in vacuum at room temperature for at least 16 h. The films were then dissolved into a buffer (HEPES 20 mM, NaCl 140 mM, pH 7.4, or 50 mM pH 7.0) to a concentration of 1 mg/mL and were thoroughly agitated at 50 °C for 30 min. The resulting multilamellar vesicle suspensions (MLVs) were then submitted to three freeze and thaw cycles (from liquid nitrogen to 50 °C). In the case of POPC/POPE (9:1) and DMPC/DMPE (9:1) mixtures, MLVs were extruded (21 times) through a polycarbonate filter (100 nm) using a mini-extruder device (Avanti Polar Lipids) to obtain Large Unilamellar Vesicles (LUVs). Finally, lipid concentrations were determined by phosphate quantification [37].

2.4. Preparation of nanodiscs suspensions

In the case of POPC and POPC/PIP_2 (80:20% mol) nanodisc suspensions, an appropriate amount of SMA (3,1) was added to reach a final volume of 300 μL. The complete solubilisation of the membranes was verified by DLS and was confirmed when the suspensions gave rise to a monodisperse population with a size of 10–20 nm. All nanodiscs suspensions were stored in 1.5-mL Eppendorf tubes at 4 °C until use.

2.5. Production and purification of K18 peptide

pNG2 K18 (kindly given by Pr. E. Mandelkow) was used to transform *E.coli* C41 (DE3) (F- ompT hsdSB (rB- mB-) gal dcm (DE3)). Several transformants were grown on 120 mL LB + 1% dextrose, 100 mg/L ampicillin. When the culture reached an OD_{650} = 5.2, 10 mL were added to 990 mL of ZYM 5052 medium (1% N-*Z*-amine, 0.5% yeast extract, 25 mM Na_2HPO_4, 25 mM KH_2PO_4, 50 mM NH_4Cl, 5 mM Na_2SO_4, 2 mM $MgSO_4$, 0.5% glycerol, 0.05% dextrose, 0.2% lactose) containing 100 mg/L ampicillin and incubated overnight at 37 °C. After centrifugation, cell pellets (corresponding to 500 mL OD_{650} = 10) were suspended in 50 mL of MES pH 6.8 (20 mM), NaCl (500 mM), EDTA (1 mM), PMSF (1 mM), benzamidine (2 mM) and DTT (5 mM), sonicated four times (1 min cycle on ice; output 5, 50% duty cycle) and then heated at 80 °C for 20 min. After centrifugation (30 min at 15,000*g*) the supernatant was dialyzed for at least 16 h at 4 °C against cation exchange buffer A (20 mM MES pH 6.8, EDTA 1 mM, NaCl 50 mM, DTT 1 mM) with a Spectra/Por Dialysis Membrane (MWCO 3 500). The dialysate was then cleared (30 min, 15,000*g*), filtered through a 0.22 μm membrane and applied on a HiTrap SP column (GE Healthcare) equilibrated with the cation exchange buffer A. After washing with 25 mL of the same buffer, the peptide was eluted with 25 mL of Buffer B (MES 20 mM pH 6.8, EDTA 1 mM, NaCl 150 mM) and the 5-mL fractions containing most of K18 were pooled and concentrated by ultrafiltration devices (*e.g.*, Ultrafree, Millipore 5 kDa MWCO) to a final volume of 0.5 to 1 mL. Finally, the concentrated peptide was applied onto a gel filtration column (Superdex-75) equilibrated in 100 mM ammonium acetate containing 2-mercaptoethanol (0.1%). The fractions containing the pure peptide were pooled, aliquoted and lyophilized.

2.6. Dynamic light scattering

DLS measurements were performed on a Vasco Nanoparticle Size Analyser (Cordouan Technologies, France) working with a He-Ne laser (633 nm) and a detection angle of 135°.

2.7. Negative staining for transmission electron microscopy

For EM grid preparations, the sample suspension diluted at 50 μg/mL for LUVs or 2 μg/mL for nanodiscs in HEPES buffer (50 mM pH 7.0) was applied to a glow-discharged carbon-coated copper 300 mesh grids and stained with 2% uranyl acetate (w/v) solution. Images were recorded under low-dose conditions on transmission electron microscope (Tecnai F20 or CM120, ThermoFischer) using a ThermoFisher Eagle 4k_4k or a GATAN UltraScan 1000 2k_k camera. Images were analysed with ImageJ.

2.8. Microfluidic diffusional sizing

The concentrations of POPC/POPE (9:1) and DMPC/DMPE (9:1) LUVs solutions after extrusion procedure ranged from 0.2 to 1 mM. Aliquots of SMA (3:1) stock solution (11 mM) or diluted one (1.1 mM) were added to the required volume of LUVs to obtain the appropriate molar ratio ($n_{SMA3:1}/n_{Lipids}$) typically ranging from 0.001 to 100. The mixtures were incubated for at least 16 h at 25 °C for POPC/POPE (9:1) and 30 °C for DMPC/DMPE (9:1). A volume of 7 μL of SMA (3,1)/LUVs mixture was pipetted onto microfluidic chips, which were then loaded into the Microfluidic Diffusional Sizing (MDS) device Fluidity-One (Fluidic Analytics, Cambridge, UK) for measurements. The device was set to the 2–20 nm size-range setting resulting in a measurement time of 15 min.

2.9. Peptide/nanodiscs interactions

The concentration of K18 was kept constant at 1 μM. Aliquots of nanodisc solution were added to obtain lipid concentrations ranging from 1 to 50 μM into a total volume of 200 μL. The tubes were thoroughly vortexed for 30 s at room temperature and an aliquot of 7 μL of the mixture was then applied onto the microfluidic chip for size measurements by MDS.

3. Results & discussion

3.1. Protocol setup for lipid detection by MDS

In this work, we propose to use MDS to follow SMALP formation by solubilisation of lipid bilayers and to evaluate to which extent we can obtain information on such process. It is worth noticing that, MDS was designed to detect and measure protein hydrodynamic radii, in consequence, the experimental protocol must be adapted. Indeed, with MDS, protein size and concentration are determined through diffusion of the sample under laminar flow in a microfluidic chip. Briefly, the sample protein flows in channel A (ChA) running alongside a channel B (ChB) filled with water. Since no convection occurs at the interface between both channels, the protein can only migrate from channel A to channel B through diffusion, which depends on the protein size. At the end of the run, both channels are split and the protein that is left in channel A and the protein that has migrated in channel B are quantified thanks to a latent labelling specific of primary amine functions (Fig. 1).

The length of the diffusion channel on the chips used for protein sample diffusion has been tuned to detect species with a hydrodynamic radius (R_H) ranging from 0.3 to 20 nm. Thus, species with a R_H > 20 nm are not expected to be detected in ChB. In order to follow SMALP formation by MDS in a rigorous manner, we have determined four requirements that the studied system must fulfil. (1) In order to avoid underestimation of the copolymer concentration for the onset of solubilisation and overestimation for the complete solubilisation we have chosen to solubilise LUVs of homogenous diameter over MLVs [29]. Indeed, due to their onion-like concentric lipid bilayers, not all MLVs lipids are simultaneously available for solubilisation by the copolymer causing misestimations (2) To be detectable, the sample must switch from a non-diffusive to a diffusive behaviour in the microfluidic channel upon SMA (3:1) copolymer addition (note that we will refer later to diffusive and non-diffusive behaviour regarding diffusion along the microfluidic channel). In this respect, LUVs of a mean hydrodynamic radius much larger than 20 nm, are not expected to diffuse whereas the smaller nanodiscs species with expected R_H in a range between 5 and 15 nm will be detectable in channel B. (3) Again, to be detectable, the measured sample must carry a free primary amine function. Usually lysine residues or N-terminal amine functions are used in protein samples. In our case, we have doped POPC and DMPC lipids with their amino-terminated counterparts POPE and DMPE (at a mass ratio POPC/POPE and DMPC/DMPE of 9:1) in order to apply the same instrument capability to detect lipids that was used for proteins. Note that this labelling protocol also works with POPS, (1-palmitoyl-2-oleoyl-*sn*-glycero-3-phospho-L-serine) (Fig. S1) (4) since we no longer deal with pure lipid composition but with mixtures, we have to make sure that the copolymer will solubilise either lipids without preference. Indeed, SMA (3,1) has been shown to solubilise lipids in a non-selective manner allowing the use of lipid mixtures and ensuring a non-biased detection [22,36].

3.2. Validation of lipid detection by MDS

With those requirements in mind, we have performed several control experiments to validate this novel application of the MDS technology. POPC/POPE (9:1) and DMPC/DMPE (9:1) MLVs were prepared

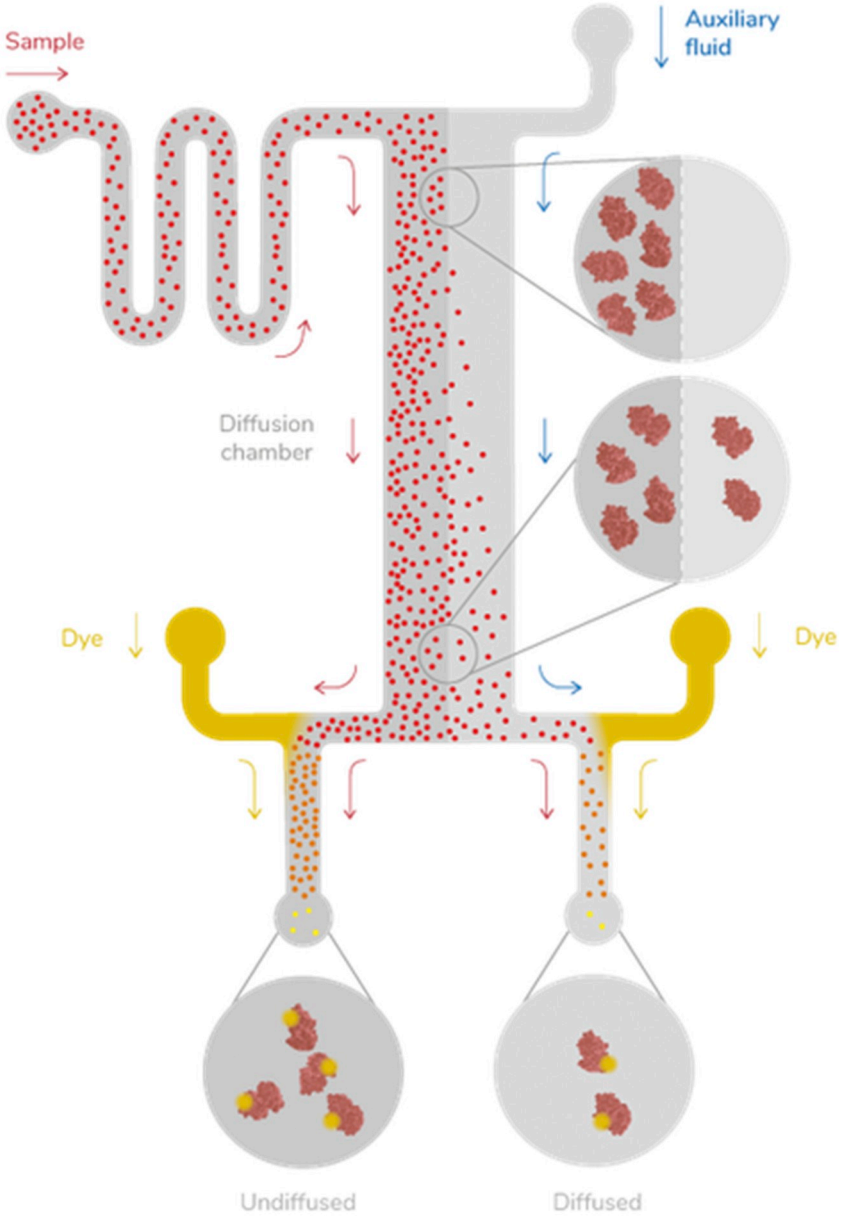

Fig. 1. Scheme representing the flow of sample through a microfluidic chip during MDS analysis on a Fluidity One instrument.

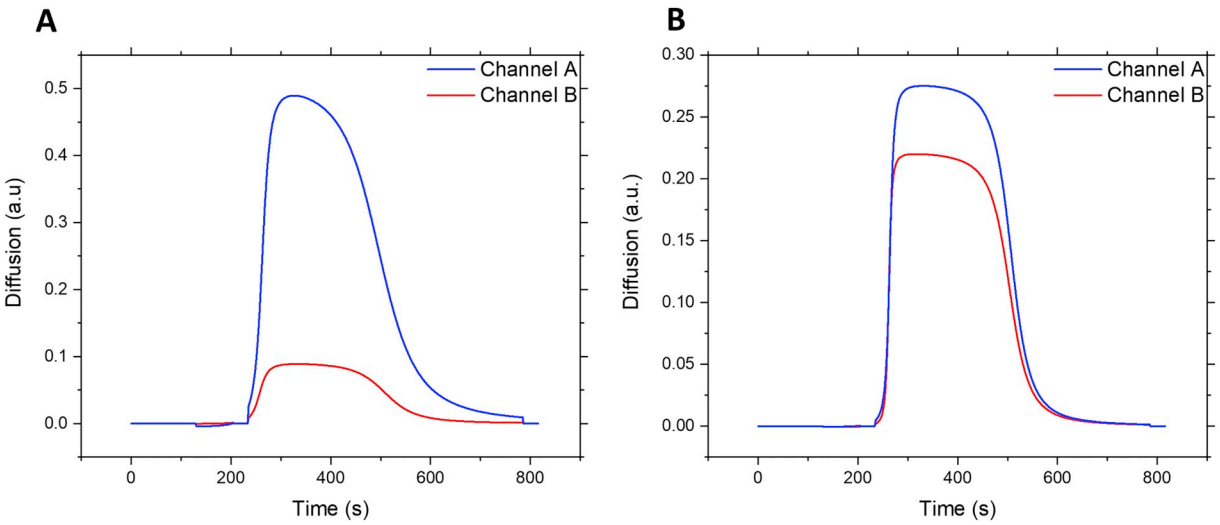

Fig. 2. A) MDS measurement of POPC/POPE (9:1) LUVs. B) MDS measurement of POPC/POPE (9:1) LUVs after solubilisation with excess SMA (3:1) ($n_{SMA3:1}/n_{Lipids} > 5$). In blue, Channel A corresponds to the channel where the sample has been introduced while in red, channel B is the one into which the sample has diffused.

at a concentration of 1 mg/mL in HEPES buffer 50 mM, pH 7.0. From those lipid suspensions, we prepared LUVs through extrusion with 100 nm diameter filter to generate homogeneous species expected to have a non-diffusive behaviour. The mean diameter of these extruded LUVs of POPC/POPE (9:1) and DMPC/DMPE (9:1) was measured by DLS, giving values of 140 and 150 nm respectively.

As expected, due to their large R_H of about 70–75 nm, twice the MDS detection limit ($R_H > 20$ nm), only a very weak diffusion signal was observed in ChB (Fig. 2A). Accordingly, the MDS instrument does not provide a value for R_H of the LUV sample as the experimental errors would be too large (note that the same experiment with MLVs, which diameter is around 700 nm, showed no diffusion signal at all, see Fig. S1). When a large excess of SMA (3:1) was added to the LUVs ($n_{SMA3:1}/n_{Lipids} > 5$) and left to react for at least 16 h, a marked diffusion signal was observed in ChB, demonstrating that diffusion occurred for lipid particles with R_H lower than 20 nm (Fig. 2B).

In order to support the results obtained with MDS, it is highly desirable to correlate them with a visual record of the lipid samples. In this respect, the samples were observed by transmission electron microscopy (Fig. 3A and B). The LUVs exhibited dimensions with an average diameter of 150 ± 40 nm and 150 ± 12 nm for POPC/POPE (9:1) and DMPC/DMPE (9:1), respectively, in agreement with the DLS measurements. After exposition to excess of SMA (3:1) overnight at 25 °C for POPC/POPE (9:1) and 30 °C for DMPC/DMPE (9:1), LUVs were solubilised into nanodisc shaped particles with a diameter of 10.5 ± 0.7 nm and 11.7 ± 0.9 nm for each composition respectively (Fig. 3C). These values are in good agreement with their typical diameter of ~10 nm reported in the literature [26,36,38]. Importantly, the observed mean diameters of the objects correlate perfectly both with their diffusive behaviour (nanodiscs) or non-diffusive behaviour (LUVs) observed by MDS. This set of control experiments following our established protocol proved that MDS can (1) detect lipids in addition to protein and (2) can distinguish between LUVs and nanodiscs due to their different size range.

Solubilisation of POPC/POPE (9:1) and DMPC/DMPE (9:1) LUVs by SMA (3:1).

The validation of this approach following the results described above invited us to further explore the SMALPs formation by MDS. We asked ourselves the questions if, beyond the extraction of nanodiscs size, it would be possible to access the concentration of copolymer required for the onset of solubilisation, R_{sat}, and for the complete solubilisation, R_{sol}, of lipids. Thus, we have explored the solubilisation of LUVs composed of POPC/POPE (9:1) (long alkyl chains 16:0–18:1) and DMPC/DMPE (9:1) (short alkyl chains 14:0) induced by SMA (3:1) copolymer. Our objective, besides further exploring MDS capabilities was to determine whether lipid chain unsaturation could affect the values of R_{sat} and R_{sol}. As LUVs were prepared by extrusion, we have systematically determined the lipid concentrations with phosphorus assays [37]. Typically, LUVs concentrations ranging between 0.2 and 1 mM were measured. Increasing amounts of SMA (3:1) copolymer

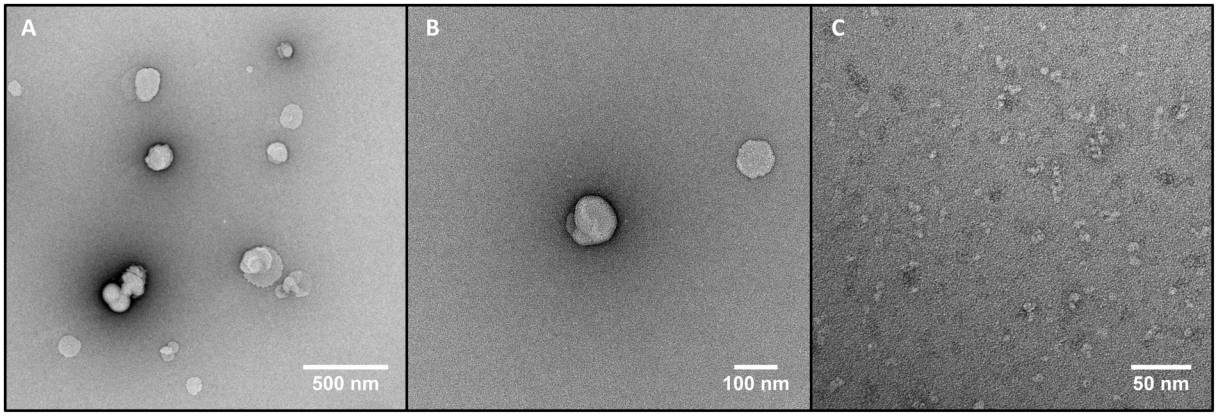

Fig. 3. A and B) TEM images of LUVs of POPC/POPE (9:1) and C) after addition of solubilising excess SMA (3:1) ($n_{SMA3:1}/n_{Lipids} > 5$).

were added to the required volume of LUVs solutions to obtain the desired ratio. Samples were incubated for at least 16 h at 25 °C for POPC/POPE (9:1) and 30 °C for DMPC/DMPE (9:1), to avoid impact of membrane fluidity changes on the process.

The molar ratio $n_{SMA3:1}/n_{Lipids}$ was explored extensively from values as low as 0.001 up to 100. After MDS measurements, the diffusion profiles of ChA and ChB were extracted and their maxima of intensity were used to define a diffusion ratio equal to $I_{max(ChB)}/(I_{max(ChA)} + I_{max(ChB)})$. This so-defined diffusion ratio can vary between two extrema, 0 and 0.5. The absence of diffusion corresponds to a value of 0 while a value of 0.5 means that equilibrium has been reached between both channels and the samples have fully diffused. Measurements for each molar ratio were at least duplicated ($n \geq 2$). For each lipid mixture, the diffusion ratio $I_{max(ChB)}/(I_{max(ChA)} + I_{max(ChB)})$ has been plotted against the molar ratio $n_{SMA3:1}/n_{Lipids}$ (Fig. 4A and B). R_{sat} and R_{sol} values were determined by linear fitting of $I_{max(ChB)}/(I_{max(ChA)} + I_{max(ChB)})$ *vs* $n_{SMA3:1}/n_{Lipids}$ following a three stages solubilisation process as described in [36,39]. Briefly, in stage I the diffusion ratio remains constant before R_{sat}. In stage II, the diffusion ratio increases from R_{sat} with a steep slope until reaching a plateau marking R_{sol} and the beginning of stage III, see supplementary data (Fig. S2).

In the case of POPC/POPE (9:1) mixture, for molar ratios below 0.070, the diffusion ratio has a constant value around 0.1, similar to the diffusion ratio observed in the absence of SMA (3:1). This means that for molar ratios ≤0.070, the diffusion behaviour remained unaffected, corresponding to stage I in the three-stage solubilisation model where LUVs start to be loaded with copolymer molecules. For molar ratio ≥ 0.070, the diffusion ratio started to increase with a steep slope. Interestingly this molar ratio matched quite well the saturation ratio (R_{sat} = 0.108) for pure POPC LUVs solubilised by SMA (3:1) determined by the Keller's group using ^{31}P NMR [36] (Table 1). In the case of DMPC/DMPE (9:1) mixture, the diffusion ratio remained constant at a slightly higher value of 0.12 than POPC/POPE (9:1) for molar ratio below 0.043. Above 0.043, the diffusion ratio started to increase significantly. Again this value is in good agreement with the R_{sat} = 0.078 reported for pure DMPC [36] (Table 1). In this respect, the increase of diffusion ratios for both lipid mixtures marked the onset of solubilisation and the beginning of stage II. Interestingly, MDS was able to distinguish between the solubilisation of saturated (DMPC/DMPE) and unsaturated (POPC/POPE) lipids giving distinct R_{sat} values of 0.043 *vs* 0.070 respectively. For POPC/POPE 9:1, a further increase in SMA (3:1) concentration led to a plateau at a diffusion ratio value of 0.45 close to the theoretical equilibrium value of 0.5. The plateau appeared at molar ratio ≥ 1.03. This value is very different from the R_{sol} reported previously for POPC (R_{sol} = 0.167) (Table 1). For DMPC/DMPE 9:1, increasing further the molar ratio $n_{SMA3:1}/n_{Lipids}$ allowed to reach a plateau for molar ratio > 0.42, which is once again much higher than the reported R_{sol} for pure DMPC (R_{sol} = 0.144) [36] (Table 1). These values, that could have been anticipated as a direct reading of the complete solubilisation ratio at the beginning of stage III were however larger than R_{sol} values reported in the literature (Table 1). Thus, we will refer later to these noticeably high values as "apparent R_{sol}".

Table 1
Comparative table of R_{sat} and R_{sol} values for SMA (3:1) driven solubilisation of different lipids or mixtures.

	R_{sat}		R_{sol}		R_{sol}^{30nm} [c]	
	^{31}P NMR	MDS	^{31}P NMR	MDS	^{31}P NMR	MDS
POPC	0.108[a]	–	0.167[a]	–	–	
DMPC	0.078[a]	–	0.144[a]	–	–	
POPC/POPE (9:1)	*0.1*[a]	0.07	*0.175*[a]	1.03[b]	–	0.36
DMPC/DMPE (9:1)	–	0.043	–	0.42[b]	–	0.17

[a] Values taken or *extrapolated* from [36].
[b] Apparent R_{sol}.
[c] $n_{SMA3:1}/n_{Lipids}$ ratio for which nanodiscs of 30 nm diameter were observed.

Our results indicate that the approach used apparently slightly underestimate R_{sat} values whereas they largely overestimate R_{sol} values. Two reasons can explain these observed discrepancies. First, R_{sat} and R_{sol} values were compared to the ones determined for pure POPC or DMPC LUVs whereas we have introduced a small fraction of POPE or DMPE to enable sample detection. The introduction of such lipids is not without consequence. Due to their smaller phosphoethanolamine headgroups, POPE and DMPE present intrinsic negative curvature, inducing an increased lateral pressure in the bilayer. The introduction of lipids with negative curvature has been shown to greatly influence the solubilisation by SMA copolymer. In the case of DOPC, the introduction of a fraction of DOPE seems to facilitate the beginning of solubilisation, but prevents complete solubilisation [19]. This observation was further complemented by another study, demonstrating that the introduction of POPE in POPC bilayers tends to decrease R_{sat} values while at the same time increasing R_{sol} values, meaning that more SMA (3:1) copolymer is required to reach complete solubilisation [36]. Importantly, no bias was observed in the solubilisation of POPE over POPC, indicating that the global state of the bilayer governs the solubilisation rather than the individual properties of each lipid component. Indeed, thanks to the quantitative results obtained in the latter study, the expected values for

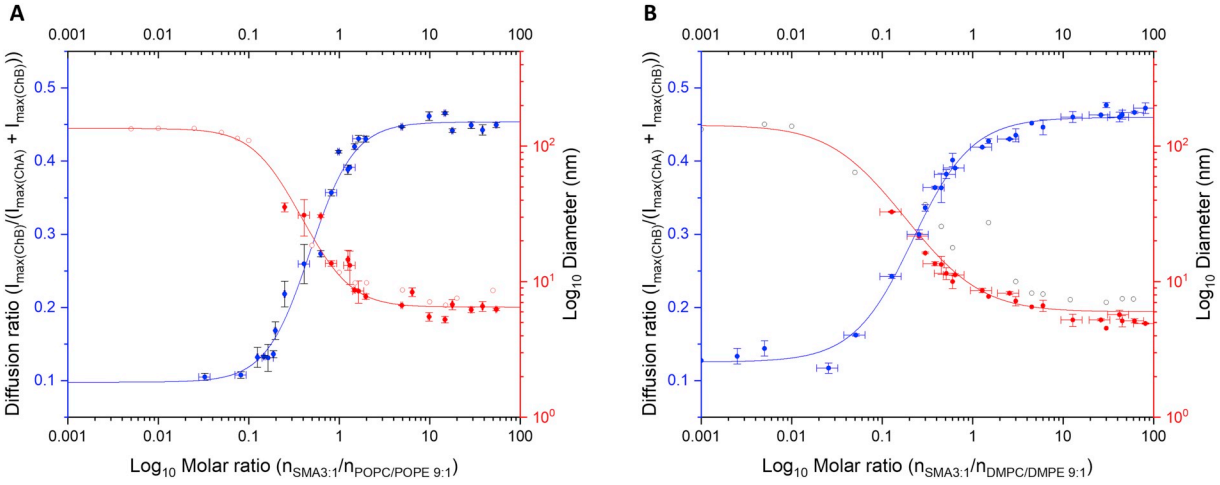

Fig. 4. Particle diffusion ratio (blue full circles) and diameter (red full circles for MDS and empty circles for DLS) as a function of the molar ratio for A) POPC/POPE (9:1) and B) DMPC/DMPE (9:1). Horizontal blue and red error bars represent variations in lipid concentration determination. Vertical blue and red bars represent the standard deviation on the measurements ($n \geq 2$). Particle diameters were calculated by multiplying by two R_H values obtained by MDS.

R_{sat} end R_{sol} for the solubilisation of POPC/POPE (9:1) by SMA (3:1) can be estimated around ~ 0.1 (0.108 without POPE) and ~ 0.175 (0.167 without POPE) respectively. Consequently, the presence of PE in our systems supports the slightly lower values of R_{sat} that we have observed, but is hardly compatible with the large increase that we have measured for R_{sol} values.

In this respect, a second observation could explain our apparent overestimation of the R_{sol} values. Indeed, to reach complete solubilisation, more and more copolymer molecules were added to the solution competing for a finite amount of lipids. It has been shown that increasing amount of copolymer tends to decrease the size of nanodiscs [36,39]. Indeed, we have determined apparent R_{sol} from the maximum values of the diffusion ratio, which depended on the size of the nanodisc. Therefore, the size reduction of SMALPs diameter as a function of the copolymer concentration could explain the overestimation of the R_{sol} value. In this respect, we have plotted the diameters of diffusing particles detected by MDS against the molar ratio (Fig. 4A and B). Notably, the following interpretation of R_{sol} values is based on the assumption that all LUVs have been converted into nanodiscs, an information that MDS is unfortunately not able to provide. Interestingly, our results show that the usual size range of nanodiscs of 10–30 nm is reached for molar ratios preceding the beginning of the plateau of the diffusion ratio curve, in other words before the apparent R_{sol}. Typically, SMALPs with diameters of 30 nm are obtained for molar ratios of ~ 0.36 for POPC/POPE (9:1) and ~ 0.17 for DMPC/DMPE (9:1). Those latter values reported as $R_{sol}^{30\ nm}$ in Table 1 are much closer to the R_{sol} values reported in the literature. Diameters of 10 nm are observed for larger molar ratio values ($R_{sol}^{10\ nm}$) of 1 and 0.72 for POPC/POPE (9:1) and DMPC/DMPE (9:1) respectively. For both lipid mixtures, increasing further the molar ratio leads to a plateau with a lower limit at ~ 6 nm diameter, which seems to be the lowest achievable diameter for SMA (3:1) based SMALPs.

Additionally, DLS measurement were performed to compare with MDS data. Despite a slight overestimation, the diameters determined by DLS were in good agreement with the ones measured by MDS (Fig. 4A and B). While DLS is known to be biased toward large particles because of the 10^6 factor between the light diffusion and particle size, our measurements did not detect large particles (diameter > 100 nm) in the molar ratio range where MDS is able to determine particle size (R_H 0.3–20 nm). This observation tends to support: (1) the assumption that all LUVs were converted into nanodiscs (2) the observation that the size of nanodiscs decreased with increasing copolymer concentration. Consequently, MDS is efficient in the determination of R_{sat}, namely the onset of solubilisation, with values that are very similar to those reported in the literature. However, regarding R_{sol} determination, the dependence of the particle size appears to lead to larger values than those obtained by ^{31}P NMR. Nevertheless, MDS provides a relevant range for R_{sol} values and offers the opportunity to carefully control SMALPs size once R_{sol} is reached by fine-tuning the $n_{SMA3:1}/n_{Lipids}$ ratio.

3.3. Peptide/nanodisc interactions

As an additional application of MDS to illustrate its potential, we studied the interaction of a peptide with SMALPs of different compositions. In this case, the lipids used (POPC and PIP_2) do not contain primary amines, and the technique specifically follows peptide diffusion. Aggregation of phosphorylated Tubulin-associated unit (Tau) protein is involved in the neurodegeneration process observed in Alzheimer's disease [40]. This phenomenon appears as a pathological event and needs to be investigated. In particular, negative lipids have been highlighted to induce Tau protein aggregation thus suggesting the importance of such lipids in the interaction [41–44]. This phenomenon stems from the aggregative domain (K18) of Tau, known as the microtubule-binding domain [45]. In a recent study, we have demonstrated that PIP_2, a negatively charged lipid found in the inner leaflet of membranes, promoted K18 peptide aggregation and fibrillation [46].

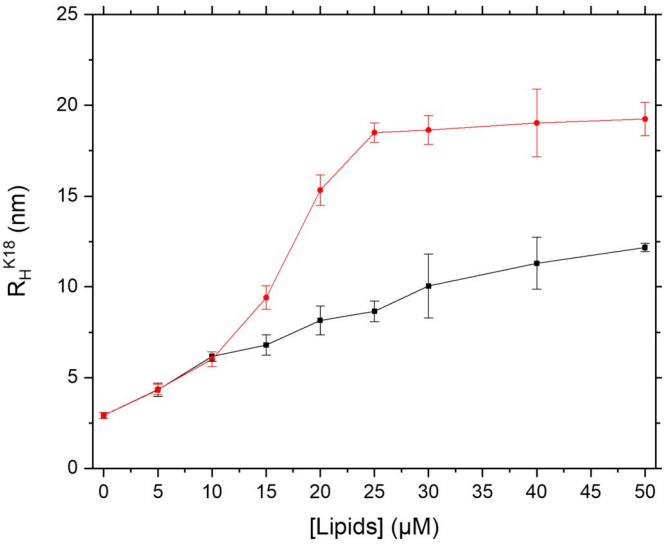

Fig. 5. Hydrodynamic radius (R_H) changes of K18 (1 μM) following a titration with increasing concentrations of POPC (black) and POPC/PIP_2 (80/20 mol%) (red) SMALPs. Each experiment was repeated three times to get statistical insight about the size variation upon SMALP interaction.

To investigate the specific interaction with PIP_2, we prepared POPC and POPC/PIP_2 (80/20%mol) SMALPs with sizes of 9.3 nm and 10.5 nm respectively (determined by DLS). Without lipids, K18 exhibited a mean native hydrodynamic radius of 2.9 ± 0.1 nm as measured by MDS. In aqueous solution, the peptide is supposed to be unfolded [47]. Pure zwitterionic lipids such as POPC have been shown to be unable to promote K18 aggregation [46]. Yet, we observed a progressive increase in size of the peptide hydrodynamic radius up to 12.2 ± 0.2 nm in the presence of 50 μM of lipids (Fig. 5). In addition, measurements of K18 with SMA (3:1) copolymer in absence of lipids (to a copolymer concentration equivalent to 25 μM of SMALPs) showed an increase of K18 radius to 5.2 nm. Such results are pointing to an interaction between K18 and the copolymer molecules. The peptide is positively charged at physiological pH [43] and can establish electrostatic interactions with the maleic acid moieties of the copolymer that are partially deprotonated at pH 7.4 [22]. By contrast, in presence of PIP_2-containing nanodiscs, K18 size evolution was different as the diameter increase was much more pronounced for same lipid concentrations (above 10 μM). A maximum hydrodynamic radius of 19.2 ± 0.9 nm was reached at 50 μM lipid POPC/PIP_2 concentration. It should be pointed out that this value corresponds to the maximum radius value measurable with the current set-up and, therefore, the plateau reached for lipid concentrations ≥25 μM indicated that the radius of the resulting objects was ≥20 nm. Two co-existing phenomena could be responsible for this substantial increase in the hydrodynamic radius of K18: (1) K18 interactions with PIP_2-containing nanodiscs, (2) aggregation of K18 peptides promoted by the presence of PIP_2. This phenomenon was observed within few minutes after mixing the peptide and the nanodiscs, a short time scale relative to the onset of fibrillation of K18, which was reported to be few hours of incubation in the presence of lipids [46]. The technique may therefore probe preliminary events that eventually lead to the formation of fibers induced by negatively charged lipids such as PIP_2. The formation of the first aggregated objects (a few monomers) constitute a crucial event that is generally not temporally characterised, as they are not detected with classical methods such as fluorescence assays. The formation of small peptide aggregates is of primary importance, as it may trigger nucleation and lead to the formation of fibers.

4. Conclusions

With their undeniable assets in the study of membrane proteins over conventional detergents, SMALPs draw more and more attention from structural biologists, biophysicists and chemists. With the idea of pushing forward the boundaries set by the current inherent limitations of SMALPs, many variants have been developed. Such an emulation calls for better characterisation and control of SMALPs formation, a process that remains to be understood in detail. In this work, we have used a novel method based on microfluidic diffusional sizing to follow SMALPs formation from SMA (3:1)-driven solubilisation of LUVs composed of POPC/POPE (9:1) and DMPC/DMPE (9:1) mixtures. While this technology was originally developed to detect and measure protein hydrodynamic radius mostly for quality control purposes, herein we have set up a protocol to follow SMALPs formation. We have demonstrated that the introduction of a small fraction of amino-containing lipids enabled the detection of lipid particles. This opens the road to detect virtually any primary amine-containing molecule, emphasizing the versatility of the technique. Consequently, using minute amount of sample (<10 μL) and in a relative short time (t < 15 min) MDS was able to determine the diameter of SMALPs with high precision as confirmed by supportive DLS data. Taking advantage of MDS diffusion profiles derived from the titration of LUVs by SMA (3:1) copolymer, we were able to construct saturation curves providing a direct reading of the solubilisation process. The onset of solubilisation (R_{sat}) can be obtained directly from the curve. Interestingly, MDS is also sensitive to the subtle effect of chain unsaturation revealing slightly different R_{sat} values for POPC and DMPC in agreement with the literature. However, since SMALPs diameter keeps decreasing after complete solubilisation upon SMA (3:1) addition, MDS profiles still evolved even after complete bilayer solubilisation, causing an apparent overestimation of R_{sol}. Once this phenomenon is understood, R_{sol} values can be derived for specific SMALPs size using particle diameter *vs* molar ratio curves. In addition, once complete solubilisation is reached, MDS allows to control nanodiscs size by fine-tuning $n_{SMA3:1}/n_{Lipids}$ ratio. We demonstrate that MDS is also an effective technique to probe the first stages of fibrillation (binding to PIP_2-containing nanodiscs and/or peptide self-aggregation) by highlighting an increase in the size of K18 peptide in the presence of PIP_2 lipids. It is worth mentioning that conventional Thioflavin T-based fibrillation assays are failing to probe such early events due to their inherent small size.

Supplementary data to this article can be found online at https://doi.org/10.1016/j.bbamem.2020.183215.

Declaration of competing interest

The authors declare that they have no known competing financial interests or personal relationships that could have appeared to influence the work reported in this paper.

Acknowledgments

The authors are thankful to Sandro Keller for fruitful exchanges. M.A. is gratefully acknowledges the financial support of the Faculté des Etudes Supérieures et Post-doctorales (FESP) from Université de Montréal, of the Natural Sciences and Engineering Research Council (NSERC), of Canada, the Fonds Québécois de la Recherche sur la Nature et les Technologies (FQRNT), through its excellence network program supporting the Québec Centre for Advanced Materials, Université de Bordeaux's Initiative d'Excellence (IdEx) and Mitacs Globalink.

References

[1] Z. Cournia, T.W. Allen, I. Andricioaei, B. Antonny, D. Baum, G. Brannigan, N.-V. Buchete, J.T. Deckman, L. Delemotte, C. del Val, R. Friedman, P. Gkeka, H.-C. Hege, J. Hénin, M.A. Kasimova, A. Kolocouris, M.L. Klein, S. Khalid, M.J. Lemieux, N. Lindow, M. Roy, J. Selent, M. Tarek, F. Tofoleanu, S. Vanni, S. Urban, D.J. Wales, J.C. Smith, A.-N. Bondar, Membrane protein structure, function, and dynamics: a perspective from experiments and theory, J. Membr. Biol. 248 (2015) 611–640.
[2] R. Phillips, T. Ursell, P. Wiggins, P. Sens, Emerging roles for lipids in shaping membrane-protein function, Nature 459 (2009) 379.
[3] D.J. Scott, L. Kummer, D. Tremmel, A. Plückthun, Stabilizing membrane proteins through protein engineering, Curr. Opin. Chem. Biol. 17 (2013) 427–435.
[4] P. Champeil, S. Orlowski, S. Babin, S. Lund, M. le Maire, J. Møller, G. Lenoir, C. Montigny, A robust method to screen detergents for membrane protein stabilization, revisited, Anal. Biochem. 511 (2016) 31–35.
[5] A. Sadaf, K.H. Cho, B. Byrne, P.S. Chae, Chapter four - amphipathic agents for membrane protein study, in: A.K. Shukla (Ed.), Methods in Enzymology, Academic Press, Place Published, 2015, pp. 57–94.
[6] J.H. Kleinschmidt, J.-L. Popot, Folding and stability of integral membrane proteins in amphipols, Arch. Biochem. Biophys. 564 (2014) 327–343.
[7] U.H.N. Dürr, R. Soong, A. Ramamoorthy, When detergent meets bilayer: birth and coming of age of lipid bicelles, Prog. Nucl. Magn. Reson. Spectrosc. 69 (2013) 1–22.
[8] I. Marcotte, M. Auger, Bicelles as model membranes for solid- and solution-state NMR studies of membrane peptides and proteins, Concepts Magn. Reson. A 24A (2005) 17–37.
[9] T.K. Ritchie, Y.V. Grinkova, T.H. Bayburt, I.G. Denisov, J.K. Zolnerciks, W.M. Atkins, S.G. Sligar, Chapter eleven - reconstitution of membrane proteins in phospholipid bilayer nanodiscs, in: N. Düzgünes (Ed.), Methods in Enzymology, Academic Press, Place Published, 2009, pp. 211–231.
[10] J. Kern, A. Guskov, Lipids in photosystem II: multifunctional cofactors, J. Photochem. Photobiol. B Biol. 104 (2011) 19–34.
[11] M. Overduin, B. Klumperman, Advancing membrane biology with poly(styrene-co-maleic acid)-based native nanodiscs, Eur. Polym. J. 110 (2018).
[12] T.J. Knowles, R. Finka, C. Smith, Y.-P. Lin, T. Dafforn, M. Overduin, Membrane proteins solubilized intact in lipid containing nanoparticles bounded by Styrene Maleic Acid copolymer, J. Am. Chem. Soc. 131 (2009) 7484–7485.
[13] S. Rajesh, T. Knowles, M. Overduin, Production of membrane proteins without cells or detergents, New Biotechnol. 28 (2011) 250–254.
[14] T.H. Bayburt, S.G. Sligar, Membrane protein assembly into nanodiscs, FEBS Lett. 584 (2010) 1721–1727.
[15] A.C.K. Teo, S.C. Lee, N.L. Pollock, Z. Stroud, S. Hall, A. Thakker, A.R. Pitt, T.R. Dafforn, C.M. Spickett, D.I. Roper, Analysis of SMALP co-extracted phospholipids shows distinct membrane environments for three classes of bacterial membrane protein, Sci. Rep. 9 (2019) (1813).
[16] V. Schmidt, M. Sidore, C. Bechara, J.-P. Duneau, J.N. Sturgis, The lipid environment of Escherichia coli Aquaporin Z, Biochim. Biophys. Acta Biomembr. 1861 (2019) 431–440.
[17] M.G. Karlova, N. Voskoboynikova, G.S. Gluhov, D. Abramochkin, O.A. Malak, A. Mulkidzhanyan, G. Loussouarn, H.J. Steinhoff, K.V. Shaitan, O.S. Sokolova, Detergent-free solubilization of human Kv channels expressed in mammalian cells, Chem. Phys. Lipids 219 (2019) 50–57.
[18] D.J.K. Swainsbury, S. Scheidelaar, N. Foster, R. van Grondelle, J.A. Killian, M.R. Jones, The effectiveness of styrene-maleic acid (SMA) copolymers for solubilisation of integral membrane proteins from SMA-accessible and SMA-resistant membranes, Biochim. Biophys. Acta Biomembr. 1859 (2017) 2133–2143.
[19] S. Scheidelaar, M.C. Koorengevel, J.D. Pardo, J.D. Meeldijk, E. Breukink, J.A. Killian, Molecular model for the solubilization of membranes into nanodisks by styrene maleic acid copolymers, Biophys. J. 108 (2015) 279–290.
[20] J.M. Dörr, S. Scheidelaar, M.C. Koorengevel, J.J. Dominguez, M. Schäfer, C.A. van Walree, J.A. Killian, The styrene–maleic acid copolymer: a versatile tool in membrane research, Eur. Biophys. J. 45 (2016) 3–21.
[21] C. Sun, S. Benlekbir, P. Venkatakrishnan, Y. Wang, S. Hong, J. Hosler, E. Tajkhorshid, J.L. Rubinstein, R.B. Gennis, Structure of the alternative complex III in a supercomplex with cytochrome oxidase, Nature 557 (2018) 123–126.
[22] S. Scheidelaar, M.C. Koorengevel, C.A. van Walree, J.J. Dominguez, J.M. Dörr, J.A. Killian, Effect of polymer composition and pH on membrane solubilization by Styrene-Maleic Acid copolymers, Biophys. J. 111 (2016) (1974-1986).
[23] A.O. Oluwole, B. Danielczak, A. Meister, J.O. Babalola, C. Vargas, S. Keller, Solubilization of membrane proteins into functional lipid-bilayer nanodiscs using a Diisobutylene/Maleic Acid copolymer, Angew. Chem. Int. Ed. 56 (2017) 1919–1924.
[24] K. Yasuhara, J. Arakida, T. Ravula, S.K. Ramadugu, B. Sahoo, J. Kikuchi, A. Ramamoorthy, Spontaneous lipid nanodisc fomation by amphiphilic polymethacrylate copolymers, J. Am. Chem. Soc. 139 (2017) 18657–18663.
[25] T. Ravula, N.Z. Hardin, S.K. Ramadugu, S.J. Cox, A. Ramamoorthy, Formation of pH-resistant monodispersed polymer–lipid nanodiscs, Angew. Chem. Int. Ed. 57 (2018) 1342–1345.
[26] S. Lindhoud, V. Carvalho, J.W. Pronk, M.-E. Aubin-Tam, SMA-SH: modified Styrene–Maleic Acid copolymer for functionalization of lipid nanodiscs, Biomacromolecules 17 (2016) 1516–1522.
[27] P.S. Orekhov, M.E. Bozdaganyan, N. Voskoboynikova, A.Y. Mulkidjanian, H.-J. Steinhoff, K.V. Shaitan, Styrene/Maleic Acid copolymers form SMALPs by pulling lipid patches out of the lipid bilayer, Langmuir 35 (2019) 3748–3758.
[28] M. Xue, L. Cheng, I. Faustino, W. Guo, S.J. Marrink, Molecular mechanism of lipid nanodisc formation by Styrene-Maleic Acid copolymers, Biophys. J. 115 (2018) 494–502.
[29] D. Lichtenberg, H. Ahyayauch, F.M. Goñi, The mechanism of detergent solubilization of lipid bilayers, Biophys. J. 105 (2013) 289–299.
[30] D. Lichtenberg, H. Ahyayauch, A. Alonso, F.M. Goñi, Detergent solubilization of lipid bilayers: a balance of driving forces, Trends Biochem. Sci. 38 (2013) 85–93.

[31] A. Helenius, K. Simons, Solubilization of membranes by detergents, Biochim. Biophys. Acta Rev. Biomembr. 415 (1975) 29–79.
[32] E.V. Yates, T. Müller, L. Rajah, E.J. De Genst, P. Arosio, S. Linse, M. Vendruscolo, C.M. Dobson, T.P.J. Knowles, Latent analysis of unmodified biomolecules and their complexes in solution with attomole detection sensitivity, Nat. Chem. 7 (2015) 802.
[33] H. Gang, C. Galvagnion, G. Meisl, T. Müller, M. Pfammatter, A.K. Buell, A. Levin, C.M. Dobson, B. Mu, T.P.J. Knowles, Microfluidic diffusion platform for characterizing the sizes of lipid vesicles and the thermodynamics of protein–lipid interactions, Anal. Chem. 90 (2018) 3284–3290.
[34] Y. Zhang, A.K. Buell, T. Müller, E. De Genst, J. Benesch, C.M. Dobson, T.P.J. Knowles, Protein aggregate-ligand binding assays based on microfluidic diffusional separation, ChemBioChem 17 (2016) 1920–1924.
[35] T.W. Herling, D.J. O'Connell, M.C. Bauer, J. Persson, U. Weininger, T.P.J. Knowles, S. Linse, A microfluidic platform for real-time detection and quantification of protein-ligand interactions, Biophys. J. 110 (2016) 1957–1966.
[36] R. Cuevas Arenas, J. Klingler, C. Vargas, S. Keller, Influence of lipid bilayer properties on nanodisc formation mediated by styrene/maleic acid copolymers, Nanoscale 8 (2016) 15016–15026.
[37] G. Rouser, S. Fleischer, A. Yamamoto, Two dimensional thin layer chromatographic separation of polar lipids and determination of phospholipids by phosphorus analysis of spots, Lipids 5 (1970) 494–496.
[38] M. Jamshad, V. Grimard, I. Idini, T.J. Knowles, M.R. Dowle, N. Schofield, P. Sridhar, Y. Lin, R. Finka, M. Wheatley, O.R.T. Thomas, R.E. Palmer, M. Overduin, C. Govaerts, J.-M. Ruysschaert, K.J. Edler, T.R. Dafforn, Structural analysis of a nanoparticle containing a lipid bilayer used for detergent-free extraction of membrane proteins, Nano Res. 8 (2015) 774–789.
[39] A. Grethen, A.O. Oluwole, B. Danielczak, C. Vargas, S. Keller, Thermodynamics of nanodisc formation mediated by styrene/maleic acid (2,1) copolymer, Sci. Rep. 7 (2017) 11517.
[40] V.M.-Y. Lee, M. Goedert, J.Q. Trojanowski, Neurodegenerative tauopathies, Annu. Rev. Neurosci. 24 (2001) 1121–1159.
[41] S.A. Mari, S. Wegmann, K. Tepper, B.T. Hyman, E.-M. Mandelkow, E. Mandelkow, D.J. Müller, Reversible cation-selective attachment and self-assembly of human Tau on supported brain ipid membranes, Nano Lett. 18 (2018) 3271–3281.
[42] N. Ait-Bouziad, G. Lv, A.-L. Mahul-Mellier, S. Xiao, G. Zorludemir, D. Eliezer, T. Walz, H.A. Lashuel, Discovery and characterization of stable and toxic Tau/phospholipid oligomeric complexes, Nat. Commun. 8 (2017) 1678.
[43] S. Elbaum-Garfinkle, T. Ramlall, E. Rhoades, The role of the lipid bilayer in tau aggregation, Biophys. J. 98 (2010) 2722–2730.
[44] C.N. Chirita, M. Necula, J. Kuret, Anionic micelles and vesicles induce Tau fibrillization in vitro, J. Biol. Chem. 278 (2003) 25644–25650.
[45] T. Crowther, M. Goedert, C.M. Wischik, The repeat region of microtubule-associated protein Tau forms part of the core of the Paired Helical Filament of Alzheimer's disease, Ann. Med. 21 (1989) 127–132.
[46] D. Talaga, W. Smeralda, L. Lescos, J. Hunel, N. Lepejova-Caudy, C. Cullin, S. Bonhommeau, S. Lecomte, PIP2 phospholipid-induced aggregation of Tau filaments probed by Tip-Enhanced Raman Spectroscopy, Angew. Chem. Int. Ed. 57 (2018) 15738–15742.
[47] M. von Bergen, S. Barghorn, L. Li, A. Marx, J. Biernat, E.-M. Mandelkow, E. Mandelkow, Mutations of Tau protein in frontotemporal dementia promote aggregation of Paired Helical Filaments by enhancing local β-structure, J. Biol. Chem. 276 (2001) 48165–48174.